AD-A218 790

DTIC FILE COPY

GL-TR-89-0328

Optical Properties of Cometary Dust

David J. Lien

University of Arizona
Steward Observatory
Tucson, AZ 85721

29 November 1989

DTIC
ELECTE
MAR 06 1990
S E D

Scientific Report No. 5

APPROVED FOR PUBLIC RELEASE; DISTRIBUTION UNLIMITED

GEOPHYSICS LABORATORY
AIR FORCE SYSTEMS COMMAND
UNITED STATES AIR FORCE
HANSCOM AIR FORCE BASE, MASSACHUSETTS 01731-5000

90 03 05 085

"This technical report has been reviewed and is approved for publication"

(Signature)
PAUL D. LEVAN
Contract Manager

(Signature)
STEPHAN D. PRICE
Branch Chief

FOR THE COMMANDER

(Signature)
R. EARL GOOD
Director

This report has been reviewed by the ESD Public Affairs Office (PA) and is releasable to the National Technical Information Service (NTIS).

Qualified requestors may obtain additional copies from the Defense Technical Information Center. All others should apply to the National Technical Information Service.

If your address has changed, or if you wish to be removed from the mailing list, or if the addressee is no longer employed by your organization, please notify AFGL/DAA, Hanscom AFB, MA 01731. This will assist us in maintaining a current mailing list.

Do not return copies of this report unless contractual obligations or notices on a specific document requires that it be returned.

SECURITY CLASSIFICATION OF THIS PAGE

REPORT DOCUMENTATION PAGE

1a. REPORT SECURITY CLASSIFICATION UNCLASSIFIED	1b. RESTRICTIVE MARKINGS
2a. SECURITY CLASSIFICATION AUTHORITY	3. DISTRIBUTION / AVAILABILITY OF REPORT Approved for public release; Distribution Unlimited
2b. DECLASSIFICATION / DOWNGRADING SCHEDULE	
4. PERFORMING ORGANIZATION REPORT NUMBER(S)	5. MONITORING ORGANIZATION REPORT NUMBER(S) GL-TR-89-0328
6a. NAME OF PERFORMING ORGANIZATION Steward Observatory 6b. OFFICE SYMBOL (If applicable)	7a. NAME OF MONITORING ORGANIZATION Geophysics Laboratory
6c. ADDRESS (City, State, and ZIP Code) University of Arizona Tucson AZ 85721	7b. ADDRESS (City, State, and ZIP Code) Hanscom AFB MA 01731-5000
8a. NAME OF FUNDING / SPONSORING ORGANIZATION 8b. OFFICE SYMBOL (If applicable)	9. PROCUREMENT INSTRUMENT IDENTIFICATION NUMBER F19628-87-K-0045
8c. ADDRESS (City, State, and ZIP Code)	10. SOURCE OF FUNDING NUMBERS PROGRAM ELEMENT NO. 63220C; PROJECT NO. S321; TASK NO. 18; WORK UNIT ACCESSION NO. AB

11. TITLE (Include Security Classification)
Optical Properties of Cometary Dust

12. PERSONAL AUTHOR(S)
David J. Lien

13a. TYPE OF REPORT	13b. TIME COVERED	14. DATE OF REPORT (Year, Month, Day)	15. PAGE COUNT
Scientific #5	FROM _____ TO _____	1989 NOV 29	36

16. SUPPLEMENTARY NOTATION
To appear in review book from Bamburg Comet conference

17. COSATI CODES			18. SUBJECT TERMS (Continue on reverse if necessary and identify by block number)
FIELD	GROUP	SUB-GROUP	Cometary dust; Light scattering from dust; Optical properties of dust; Thermal emission from dust; Irregular particles
03	01		
03	02		

19. ABSTRACT (Continue on reverse if necessary and identify by block number)
(see next page)

20. DISTRIBUTION / AVAILABILITY OF ABSTRACT [X] UNCLASSIFIED/UNLIMITED [ ] SAME AS RPT [ ] DTIC USERS	21. ABSTRACT SECURITY CLASSIFICATION UNCLASSIFIED
22a. NAME OF RESPONSIBLE INDIVIDUAL Paul D. Levan	22b. TELEPHONE (Include Area Code) (617) 377-4550 22c. OFFICE SYMBOL AFGL/OPC

DD FORM 1473, 84 MAR 83 APR edition may be used until exhausted. All other editions are obsolete.

SECURITY CLASSIFICATION OF THIS PAGE

Optical Properties of Cometary Dust

David J. Lien

Steward Observatory

Abstract

Cometary dust is observed in a variety of ways: scattered light, thermal emission, stellar occultations, dust coma and tail morphology, radar echo's, and meteors associated with comets. To interpret these observations with respect to the physical parameters of the dust (size, shape, composition) and the properties of the dust emitting region, the physics of how electromagnetic radiation interacts with small particles must be understood.

To understand the interaction of electromagnetic radiation with matter, the measurement and interpretation of optical constants of bulk materials must be understood Classically, a material can be approximated by a series collection of bound charges with a number of resonant frequencies. The optical constants (index of refraction or dielectric constant) of a material are a measure of the ability of the material to vibrate in response to an incoming electromagnetic wave. The laboratory measurement of optical constants is very difficult, and many published optical constants may be in error. Care must be taken in choosing a set of optical constants which best represent the material being used for modelling cometary dust.

Scattering theory is usually synonymous with Mie theory, although Mie theory pertains only to spherical particles. In many cases spheres may be good approximations to the particles in the coma, but an understanding of non-spherical scattering effects is essential to determine the limitations of the spherical approximation. A variety of methods exist which, although computationally intensive, do provide insight into shape effects.

Accession For
NTIS GRA&I ☒
DTIC TAB ☐
Unannounced ☐
Justification
By
Distribution/
Availability Codes
Dist | Avail and/or Special
A-1

QUALITY INSPECTED 4

I Introduction

The paradigm for dust ejection from the nucleus of a comet is very convoluted. The production rate, ejection direction, and ejection velocity for a single dust grain will depend on the heliocentric distance and solar altitude, as well as the history of the region emitting the dust. Integrating over the emitting region, dust size, and time and including the effects of radiation pressure and the lorentz force will yield a "picture" of the dust tail and coma at a given heliocentric distance. Our problem, however, is the inverse: given observations of the dust coma and tail, what are the physical properties of the dust (composition, particle size distribution, ejection velocity, and particle shape) and the dust emitting regions (rotation rate, distribution of ejection directions, shape and size of emitting region, and history of emission)?

Cometary dust can be detected in a variety of ways: scattered solar radiation, thermal radiation, stellar occultations, meteors associated with known comets, vaporization dust spectra for sun-grazing comets, and radar echos, as well as by in situ measurements. For most comets, observations are made by ground-based instruments detecting either scattered solar radiation or thermal emission. Clearly, to solve the inverse problem, an understanding of how small grains interact with electromagnetic radiation is necessary.

In section II, the fundamental interactions between matter and electromagnetic radiation are briefly reviewed. The measurement of optical constants is covered in section III. The interaction of electromagnetic radiation with small particles (both spherical and non-spherical) is described in section IV, and applications toward remote sensing observations of comets is discussed in section V.

This review is not meant to be complete; rather, it is meant to provide a brief synopsis of a large body of knowledge, and to provide a starting point for further work.

II Interaction of Electromagnetic Radiation and Matter

The solution of Maxwell's equations for a plane wave is

$$\mathbf{E} = \mathbf{E}_0 exp(i\mathbf{k}\cdot\mathbf{x} - i\omega t)$$

where the propagation vector may be complex: $\mathbf{k} = \mathbf{k}' + i\mathbf{k}''$. In what follows, it is assumed that $\frac{\mathbf{k}'}{|\mathbf{k}'|} = \frac{\mathbf{k}''}{|\mathbf{k}''|}$, although this need not always be true (Huffman, 1989). The wave vector is related to the complex index of refraction ($k = \frac{\omega m}{c}$), where the complex index of refraction is related to the dielectric constant (ϵ) by

$$m = c\sqrt{\epsilon\mu} = \sqrt{\frac{\epsilon\mu}{\epsilon_0\mu_0}} = n + ik,$$

where μ is the magnetic permeability of the material. Note that although both the wave vector and the imaginary part of the index of refraction are both denoted by k, the context

is usually sufficient to distinguish which is meant. In free space, $\epsilon_0 = 1$, and if $\mu_0 = \mu$, then $m^2 = \epsilon$. equating real and imaginary parts yields

$$\epsilon' = n^2 - k^2 \quad \epsilon'' = 2nk$$

$$n = \sqrt{\frac{\epsilon' + \sqrt{\epsilon'^2 + \epsilon''^2}}{2}}$$

and

$$k = \sqrt{\frac{-\epsilon' + \sqrt{\epsilon'^2 + \epsilon''^2}}{2}}.$$

Bell et al (1985) have organized a table linking the different sets of optical constants for non-magnetic materials. The wave equation can be re–written as

$$\mathbf{E} = \mathbf{E}_0 exp(-\tfrac{2\pi kz}{\lambda}) exp(\tfrac{i2\pi nz}{\lambda} - i\omega t)$$

The real part of the index of refraction, n, is related to the wavelength of the radiation in the medium, and the imaginary part, k, determines the attenuation of the wave as it traverses the medium.

Optical constants — m or ϵ — are thus used to describe the interaction of electromagnetic radiation and matter. The word "constant," however, is misleading. Figure 1 shows the optical constants of magnetite (Huffman and Stapp, 1973 and Steyer, 1974). Clearly, the optical constants are anything but constant!

The real and imaginary parts of m or ϵ are not independent. They are interrelated by the Kramers-Kronig relationship (Bell, 1967, BH, Smith, 1985, Ward, 1988):

$$n(\omega) - 1 = \frac{2}{\pi} P \int \frac{\omega' k(\omega')}{\omega'^2 - \omega^2} d\omega'$$

$$k(\omega) = -\frac{2}{\pi} P \int \frac{n(\omega') - 1}{\omega'^2 - \omega^2} d\omega'$$

where $\omega = \frac{2\pi}{\lambda}$, and P is the Cauchy principle value of the integral. Similar expressions can be written relating ϵ' and ϵ'' (Bell, 1967, BH, Smith, 1985). The Kramers-Kronig relationship can be used to determine n (or k) of $k(\omega)$ (or $n(\omega)$) is known for all ω. An additional sum rule which helps constrain n is (Bell, 1967, Smith, 1985)

$$\int_0^\infty (n(\omega) - 1) d\omega = 0$$

The optical constants are a measure of the ability of the electrons in the material to oscillate when driven by an input oscillation. Lorentz first modelled this interaction in terms of classical spring constants (Bell, 1967, BH, Jensen, 1985). The results are essentially identical to those obtained quantum mechanically, although the physical meaning of the constants change somewhat. The relationship between the dielectric constant and the physical properties of the medium is

$$\epsilon(\omega) = 1 + \sum_{j=1} \frac{\omega_p f_{ij}}{\omega_{0j}^2 - \omega^2 - i\gamma\omega}$$

where $\omega_p = \frac{\mathcal{N}e^2}{m\epsilon_0}$ is the plasma frequency, $\mathcal{N}$ is the number density of oscillators, ω_0 is the characteristic frequency of the oscillator, and γ is a damping constant. Thus the optical constants over all frequencies can be reduced to a table of ω_0, ω_p, and γ for each transition. This approximation works quite well for vibrational oscillations in the infrared (BH); the high absorption near each ω_{0j} is known as a *Reststrahlen* band. A similar model for metals, which does not include the damping term γ, is referred to as the Drude model (BH, Jensen, 1985). Figure 2 shows the main characteristics of a single oscillator Lorentz model for both ϵ and m. An important point is to notice the slight shift to higher frequencies of the peak of the imaginary component of the index of refraction compared with the peak of the ϵ'' (at ω_0). This difference will be important when interpreting the emission or scattering by small particles. Figure 2 also includes a reflectance spectrum of an infinite slab at normal incidence calculated using the Fresnel equations (see discussion below).

III Optical Constant Measurements

There are almost as many different ways to measure the optical constants of materials as there are people who measure them. Good reviews of the fundamental methods used to measure optical constants in the laboratory can be found in Bell (1967), Egan and Hilgeman (1979), Pallik (1985), and Ward (1988).

The most fundamental method is simple reflectance. For normal incidence, the reflectivity, R, is related to the real index of refraction by the Fresnel reflection coefficient (Bell, 1967, Hunter, 1985):

$$R = \frac{(n-1)^2}{(n+1)^2}$$

which can be solved directly for n:

$$n = \frac{(1+\sqrt{R})}{(1-\sqrt{R})}$$

The extension to angles different from normal includes the imaginary index of refraction, k, and the polarization of the incident and reflected radiation (Hunter, 1985, Ward, 1988). Since there are now two unknowns, a minumum of two angles or two different polarizations must be measured to get a unique answer. If the slab being measured is thin, then care must be taken to measure only the first surface reflection. Additionally, the sample must be specularly reflective, ie, there should be negligible scattering from the surface. This may be done either by cleaving a crystal, or by polishing. Note however that polishing may alter the physical property of the material near the surface, which may alter the index of refraction (Bell, 1967, Ward, 1988)!

For transmission measurements, Lambert's law relates the ratio of the incident to transmitted light to the imaginary part of the index of refraction:

$$T = I/I_0 = e^{\frac{-4\pi kt}{\lambda}}$$

where t is the thickness of the slab. Interference effects become important if the slab is thin (thin slabs are needed when measuring materials with large k), and problems with obtaining a large homogeneous sample create errors in the measurement of low k materials.

A more complicated method involves the use of polarized incident light, and is known as ellipsometry (Aspnes, 1985, Ward, 1988). This method has the advantage of higher accuracy, but also is limited to spectral regions where good transmittance polarizers exist.

Other methods for single crystals are described by Bell (1967), Egan and Hilgeman (1979), Pallik (1985) and Ward (1988). A popular method is to obtain either n or k over a wide spectral range, and use the Kramers-Kronig relationship to determine the other index of refraction. This method, however, requires a high precision in the measurements, and also requires that the behavior of n (or k) be known outside the spectral bandpass.

Measurements of anisotropic materials requires the index of refraction to be measured along more than one plane. Steyer (1974) provides examples of such measurements.

A problem arises when single crystal or polished slab of a material cannot be obtained. And even if the bulk material can be obtained, often it cannot be polished smooth enough to remove the effects of scattering. For this latter case, a modified transmission theory and reflectance theory (Kubelka-Munk theory, Egan and Hilgeman, 1979) can be used along with measurements of the *total* diffuse transmitted and reflected radiation to obtain the optical constants. This method will also work with powdered samples if the size of the individual grains is much smaller than the wavelength of light (Rayleigh criterion, cf. section IV).

Besides the Kubelka-Munk method, a variety of other methods exist which allow the optical constants of powders to be obtained. Perhaps the most straight forward is to compress a powdered sample in a die until the density of the pellet approaches that of the bulk material. This usually leaves a specular reflecting surface, and normal reflectometry or ellipsometry techniques can be used (Querry, 1984, 1985, 1986). Other methods include the use of the photoacoustic effect (Schleusner, Lindberg, and White, 1975), transmittance through a KBr pellet containing the powder (Voltz, 1972, Koike et al, 1989), reflectometry coupled with effective dielectric medium theories (Gillespie and Goedecke, 1989), and various light scattering measurements (Gerber and Hindman, 1982). Toon, Pollack, and

Khare (1976) review some of these methods and discuss their strengths and weaknesses. The optical constants measured from powdered samples are often in quite good agreement with those determined from bulk samples. (Egan and Hilgeman, 1979, Querry, 1984, 1985). This is not meant to be a blanket endorsement of the accuracy of optical constants derived from powders – each set of constants must be evaluated on its own merits (if a sufficiently large spectral bandpass is available, a Kramers-Kronig analysis can be performed, and sum rules can be used to check for self consistency (Smith, 1985, Ward, 1988)).

A good example of the problems associated with measuring the optical constants of powders can be found in the book edited by Gerber and Hindeman (1980). Fifteen investigators were given samples of aerosols collected during a conference in Fort Collins, Colorado. The investigators were to determine a variety of optical parameters of identical samples of aerosols. One of the parameters to be measured was the complex index of refraction at optical wavelengths for soot, salt, and methylene blue. Variations of factors of two between investigators were common, and even order of magnitude differences were seen. Variations in the other optical parameters (albedo, specific absorption coefficient, and the absorption coefficient) also showed similar variations between investigators. Although many of the measurements were made with the particles suspended in air, a few were measured from the aerosols compressed into KBr pellets. Clearly, more work needs to be done in the area of determining the optical constants of powders.

The use of powders to determine the bulk optical constants leads to the question of "what is the meaning of the optical constants derived from powders of anisotropic materials?" For example, the optical constants for crystalline olivene have been measured in the IR by Steyer (1974), and have also been measured from a powdered sample by Mukai and Koike (1989). Crystalline olivene is an anisotropic crystal, with three different indices of refraction along the three different optical axis. The data from the data of Mukai and Koike (1989) appear to be a "blend" of the bulk measurements of Steyer. This observation suggests that there may exist a dielectric constant which is some form of an average of the dielectric constants of the bulk materials in the mix.

The existence of an "effective dielectric constant" dates back to 1904, when Maxwell-Garnett (1904) sought to explain the changes in color of a colloidal dispersion as the volume fraction of the dispersant was changed. Since then, a variety of effective dielectric constant medium theories have prospered (see Bohren and Battan, 1980 for a review, also BH). The two which seem to be the most prevalent are the Maxwell-Garnett theory (Maxwell-Garnett, 1904), and the Bruggeman theory (Bruggeman, 1935). The Maxwell-Garnett theory assumes that very small particles with dielectric constant ϵ_i are embedded in a matrix with dielectric constant ϵ_m. The, the effective dielectric constant, ϵ_{eff}, is

$$\epsilon_{eff} = \frac{(1-f)\epsilon_m + \sum_i f_i \beta_i \epsilon_i}{1 - f + \sum_i f_i \beta_i}$$

where $f = \sum f_i$ is the total volume fraction of the inclusions, where each composition, i, has a volume fraction f_i, and β_i is a shape effect parameter (BH).

The Bruggeman theory assumes that the material is composed of and aggregate of small particles, each with its own volume fraction and dielectric constant. There is no

matrix material. The effective dielectric constant for the Bruggeman theory is found by solving

$$\sum_i \frac{f_i(\epsilon_i - \epsilon_{eff})}{(\epsilon_i + 2\epsilon_{eff})} = 0$$

for the effective dielectric constant, ϵ_{eff}. The solution may not converge if the optical constants are widely disparate (Lien and Hanner, 1989).

For a two component system, the Bruggeman theory is symmetric upon interchange of the two dielectric constants, whereas for the Maxwell-Garnett theory, the effective dielectric constant depends strongly on which material is chosen as the matrix. Note too that both theories were developed under the assumption that $f_i \ll 1$, whereas they are often applied in circumstances where $f_i \sim 1$ (Mukai, 1986, Lien, 1990, Lien and Hanner, 1989). Figure 3 shows an example of the application of the Bruggeman theory to a composite clay. The optical constants of equal volume fractions of montmorillonite, illite, and kaolinite (Querry, 1984) were used as input into the Bruggeman equation. The effective dielectric constant in the form of n and k) is compared in Figure 3 with the measure dielectric constant of a compressed pellet composed of an equal mix of the three clays (Querry, 1984). In this example, the results are quite good. A similar comparison with the results of Mukai and Koike (1989) for crystalline olivene with the effective dielectric constant derived from the measurements of Steyer also show good agreement, with differences probably due to differences in the composition of the olivene used in the two laboratory measurements (Lien and Hanner, 1989).

Effective medium theories have been used to describe the optical properties of icy grains (Mukai, 1986b, Mukai, 1986c, Lien, 1990) and the thermal emission from blends of non-volatiles (Lien, 1990, Lien and Hanner, 1989).

A note of caution should be inserted here about the blind use of effective dielectric constants. Each of the various effective dielectric medium theories have their successes and failures. Unless a laboratory measurement is available for comparison, it is impossible to say if the effective dielectric constants are the "correct" dielectric constants for the material. None of the effective medium theories take into account electrical interactions between the inclusions, and so at some point, they must fail (Bohren, 1986). Effective medium theories are best used as a way to search parameter space for mixtures of materials which might be of astrophysical interest. Then, one should attempt to induce a laboratory which specializes in the measurement of optical constants to measure the mixtures of interest. An additional caveat is the extension of the effective medium theories to include the effects of the shape of the individual inclusions or electromagnetic terms other than the electric dipole term. Bohren (1986) discusses in great detail the problems with attempting to extend these theories, and points out that the extensions may rely on unphysical assumptions.

A complete list of references to published optical constants or dispersion parameters would take up half this volume. A very short list of references to optical constants currently used by cometary astronomers is presented in Table 1. The list only includes references to optical constants which are reasonably complete from the UV through the IR.

IV Optical properties of particles

The interaction of electromagnetic radiation with small particles is important in many fields of science besides astronomy, and the literature is resplendent with references to this fundamental, but important problem. Monographs by van de Hulst (1957), Kerker (1969), Deirmendjian (1969), and Bohren and Huffman (1983, BH) provide excellent tutorials on light scattering by small particles. Reviews by Huffman (1975, 1977, 1989) are specifically directed toward astronomical problems, and the review by Eaton (1984) is specifically slanted toward comets. The book edited by Schuerman (1980) contains a great deal of useful information concerning the interaction of light with irregular particles.

When electromagnetic radiation interacts with a material body, the radiation can be absorbed, diffracted, reflected, or transmitted. In dealing with the interaction of radiation with small particles, a number of terms have come into use to describe the above effects. A fraction of the energy in a beam of light incident upon a single particle will be removed from the incedent beam due to one or more of the interactions described above. Extinction of the beam is said to have occured, and the particle will have a corresponding extinction cross section, C_{ext} . A fraction of this light removed from the beam will be absorbed, and can be characterized by the absorption cross section, C_{abs} . The rest of the light must be either reflected or diffracted, commonly referred to as scattered, with a scattering cross section C_{sca} . Clearly, $C_{ext} = C_{sca} + C_{abs}$. Scattering, absorption and extinction *efficiencies* are also terms often used, and they describe the ratio of the corresponding cross section with the cross section of the projection of the shape of the particle along the direction of propogation (G). For spheres, $G = \pi a^2$, where a is the radius of the particle. Thus the scattering efficiency is $Q_{sca} = C_{sca}$ /G $= C_{sca}$ / πa^2 if the particle is a sphere. Similarly, $Q_{abs} = C_{abs}$ /G and $Q_{ext} = C_{ext}$ /G. The single scattering albedo is the ratio of the radiation removed by scattering to the total extinction: $\varpi = C_{sca}$ / $C_{ext} = Q_{sca}$ / Q_{ext} . Since most particles do not scatter light isotropically, the phase function, $P(\theta)$, describes the scattered light as a function of scattering angle. The phase function for orthogonal polarizations are usually different. The phase function is normalized to 1:

$$\int_{\Omega} \frac{P(\theta)d\Omega}{4\pi} = 1$$

A measure of the departure from isotropic emission is the first moment of the phase function:

$$g = < cos(\theta) > = \int_{\Omega} \frac{cos(\theta)P(\theta)d\Omega}{4\pi}$$

where g is referred to as the asymmetry parameter. if g > 0, the radiation is preferentially scattered in the forward direction; the radiation is scattered in the backward direction if g < 0.

Since radiation carries with it momentum, the motion of a small particle can be affected by absorption and scattering. The radiation pressure efficiency is

defined as $Q_{pr} = Q_{abs} + gQ_{sca}$. Based on the above definitions, the monochromatic intensity of light scattered into 1 steradian a distance r from a particle is

$$I = \frac{I_0 P C_{sca}}{4\pi r^2}$$

The monochromatic intensity of thermal radiation radiated into 1 steradian by a particle of radius a is

$$I = \frac{\pi B(T) C_{abs}}{4\pi r^2}$$

where B(T) is the planck function.

Reviews by Hanson and Travis (1974) and Hanner et al (1982) discuss these definitions in more detail.

Lord Rayleigh first quantified the interaction of radiation with small particles. It was later shown by Mie and Debye (cf Kerker, 1969 for a history of the sphere problem) that Rayleigh's results were identical to the small particle limit of the general problem of scattering by a spherical particle of arbitrary size. Since the wave equation is usually written in terms of the circular frequency, ω, the derivations of Mie theory are usually written in terms of the size parameter of the particle: $x = \frac{2\pi a}{\lambda}$. In terms of the size parameter, Rayleigh scatterers can be defined as particles small compared to the wavelength of light ($x \ll 1$) where the polarization of the particle is in phase with the incident radiation ($|m|x \ll 1$, BH). The radiation efficiencies for the Rayleigh scattering are:

$$Q_{sca} = \frac{8}{3} x^4 \left|\frac{m^2 - 1}{m^2 + 2}\right|^2$$

$$Q_{abs} = 4x Im\left\{\frac{m^2 - 1}{m^2 + 2}\right\}$$

$$P = \frac{1}{2}(1 + cos^2(\theta))$$

$$g = 0$$

Note that if there are no strong absorptions nearby, ie $\frac{(m^2-1)}{(m^2+2)} \approx constant$, then $Q_{abs} \propto \frac{1}{\lambda}$ and $Q_{sca} \propto \frac{1}{\lambda^4}$. For an appreciable imaginary part of the index of refraction, k, $Q_{abs} \gg Q_{sca}$. For k = 0, $Q_{abs} = 0$. The equations defining the radiation efficiencies are expressed in terms of the dimensionless size parameter, x. However, there is a difference between changing x by changing the radius versus changing the wavelength. This is because the index of refraction of real materials change as a function of wavelength. Graphs of Q_{abs} versus size parameter for a constant index of refraction must be interpreted for real materials as a plot of Q_{abs} versus size at a constant wavelength.

A question often arises as to how large a particle must be before the Rayleigh approxiamtion is no longer valid. Kerker, Scheiner, and Cooke (1978) have analyzed this answer, and find that the answer depends in a complicated way on the real and imaginary indices of refraction, as well as the scattering angle.

At the opposite end of the size spectrum for Rayleigh particles, another problem arises: at what point are the bulk optical constants no longer applicable? As the particle becomes smaller, surface effects and long range forces within the particle will change. For a metal, if the size becomes comparable to the mean free path of the electrons, then the coupling between the electromagnetic wave and the material must change from that of the bulk material. Huffman (1989) discusses this problem in great detail, and suggests a lower limit of 50Å, although the size will depend on the material in question. An example of this change from bulk properties to macromolecule properties is the dramatic decrease in the melting point of small gold particles when the size becomes smaller than about 50Å (Buffat and Borel, 1976).

Almost all theoretical work to date on the scattering and absoption of light by cometary grains has been done using Mie theory. The equations describing the Mie theory are presented in the references quoted at the beginning of this section. Bohren and Huffman (1983) also include a FORTRAN program for calculating the scattering from a sphere of arbitrary size (the upper limit to the size of the particle is set by the size of the dimensioned arrays). Programs for calculating the scattering from a coated sphere and an infinite cylinder are also include in their monograph. For large particles, Nussenzveig and Wiscombe (1980) present asymptotic expressions for Q_{sca} , Q_{ext} , and Q_{pr} for $x > 100$. Ungat, Grehan, and Gouesbet (1981) describe comparisons between geometrical optics and Mie theory for transparent spheres. Kamiuto (1988) provides expressions for the single scattering albedo and the assymetry parameter derived from geometrical optics. Bohren and Nevitt (1983) describe an approximation for Q_{abs} which can be used in situations where spectral features are not important.

The results from Mie theory, or any scattering theory, are only as good as the optical constants which are input. Great care must be taken to insure that the optical constants are appropriate to the problem at hand. For example, the optical constants derived from the measurement of a polished lunar sample will depend strongly on the method by which the polishing was effected (Ward, 1988), and will also depend on the position on the surface the optical constants were measured. These optical constants can certainly be inserted into a computer program to calculate the scattered flux or thermal emission from a spherical grain, but it is not clear how the results can be interpreted in terms of the physical properties of the dust (eg, particle size distribution, or composition).

There exist a number of problems with using Mie theory to determine the scattered or thermal radiation from a particle or an ensemble of particles. Foremost is the existence of resonances due to the high degree of symmetry of the sphere. The number of resonant modes decreases as the particle becomes more non-spherical. For a given size, wavelength, and index of refraction, the difference between the radiation efficiencies in and out of resonance can range from less than a percent to over an order of magnitude. Generally, non-spherical particles will have different values for the total cross sections (C_{abs} , C_{ext} , C_{sca}), the phase function, the asymmetry parameter, the single scattering albedo compared with a sphere of an "equivalent size." These differences between scattering by spherical and non-spherical particles are generally referred to as *shape effects*.

Laboratory measurements of non-spherical particles are usually split between two methods: microwave analogs (Greenburg, 1960; Zerull, 1976, Weiss-Wrana, 1983; Wang,

1980; Schuerman, et. al., 1981) and visible (Holland and Gagne, 1970; Pinnick, et. al., 1976; Coletti, 1984). The work by Schuerman et. al., (1981) is of particular interest because they systematically investigated the scattering from objects with a range of shapes: cylinders, prolate and oblate spheroids, disks and spheres. Visible measurements suffer in that forward and backscattering measurements are very difficult to make. Recent progress has been made by using Fraunhofer diffraction to correct for the unmeasured scattering angles (Coletti, 1984), greatly inproving the accuracy of the measured scattering cross section and phase function. In general, comparisons with non-spherical particles and Mie scattering show the following tendencies:

i. forward scattering is well approximated by Mie theory, with equal volume spheres best for $x \leq 6$ and for equal projected-area spheres for $x \geq 6$.
ii. oscillations in the radiation efficiencies and phase function are damped with respect to Mie theory, with the damping increasing with increasing departure from sphericity.
iii. non-spherical particles scatter non-polarized light more efficiently at intermediate angles ($60° - 140°$) than spheres.
iv. backscattering ($140° - 180°$) is greater than spheres for opaque particles, but less than that for spheres for transparent particles
v. scattering from orthogonal polarizations becomes more similar
vi. agreement within a factor of 2 for the radiation efficiencies, the assymetry parameter, and the single scattering albedo for $x \leq 3 - 5$, rapidly worsening for larger size parameters.

Comparisons with "equivalent spheres" becomes much more difficult as the degree of non-sphericity increases, since the definition of size parameter becomes less clear as the particle shape deviates from a sphere (Gallily, 1984).

Much work has been done in attempting to compensate for shape effects. Most of the work has gone into attempting to model non-spherical effects by a size distribution of spheres. Other methods include semi-empirical models of the phase function and analytical or numerical modelling of the scattering from non-spherical particles.

Heintzenberg and Welch (1982) have investigated the retrieval of the particle size distribution of a collection of non-spherical scatterers with a particle size distribution of spheres. They find that the effects due to composition and size distribution cannot be separated, and that the retrieved particle size distribution is best matched at small size parameters ($x < 2-3$), but large deviations from the original size distribution occur for larger size parameters. They also find that no combination of spherical scatters can describe the original phase function. These results have also been obtained by Perry, Hunt and Huffman (1978), Pinnick, Carroll, and Hofmann (1976), and Holland and Draper (1967). An interesting result from theoretical calculations using perturbation theory (Chylek, Kiehl, and Mugnai, 1979) is that for small deviations from sphericity (¡5%), the scattering from two conjugate irregular particles can be replaced by the scattering from two spheres of the radius to which the particles are conjugate. This shows that the inversion of the scattering problem is not unique.

An alternative approach is the characterization of the phase function by means of theoretical arguments matched with observations. These models are termed semi-empirical methods. Pollack and Cuzzi (1980) have produced models of non-spherical scattering by

calculating the phase function from Fraunhofer diffraction, reflected rays, and transmitted rays modified to reproduce the experimental results of Zerull (1976). Coletti (1984) introduced a similar semi-empirical method, and compared the results with his own laboratory measurements. It might be useful to apply these methods to cometary phase functions to constrain the range of permissible sizes and indices of refraction.

Most of the current research on the effects of non-sphericity have been through theoretical models of non-spherical scatterers. Theoretically, the scattering by non-spherical particles can be solved in closed form for certain shapes: spheroids (Asano and Yamamoto, 1975), infinite cylinders (BH), coated spheres (BH), and of course, spheres. Van de Hulst (1957), Kerker (1969) and BH also contain useful references to approximations for small, smooth, non-spherical particles (eg, Rayleigh-Gans approximation, Rayleigh scattering with shape effects, etc). Huffman and Bohren (1980) describe the effects of elliptical Rayleigh scatters, and show that they cannot be modelled by a size distribution of small spheres.

Since the light scattering from irregular particles can only be solved analytically for simple shapes, a large number of numerical methods have been developed to solve for the phase function and radiation efficiencies of non-spherical particles.

Perturbation methods have been developed by Yeh (1964), and an interesting point matching method has been numerically investigated by Yeh and Mei (1980).

For relatively smooth particles, the T-matrix method (Waterman, 1965) also known as the extended boundary condition method (EBCM, Barber and Yeh, 1975) have been used to investigate the scattering by non-spherical particles. The EBCM has been modified to improve convergence for very elongated particles by Werby and Chin-Bing (1985) and Iskander, Lakhtakia, and Durney (1983). Perrin and Chiappetta (1985) and Perrin and Lamy (1986) approach the problem of scattering by irregular particles through the framework of the eikonal picture.

An interesting method which shows potential is the discrete dipole method, commonly referred to as the Purcell-Pennypacker method (Purcell and Pennypacker, 1973). This method has been applied to a variety of problems (cf Singham and Bohren, 1989; Iskander, Chen, and Penner, 1989; Kattawar and Humphreys, 1980; Berry and Percival 1986; Drolen and Tien 1987; and Goedecke and O'Brien, 1988), and with proper precautions, can supply quantitative results. This model has been applied to astronomical problems by Draine (1988) and Wright (1989).

The results from numerical calculations are consistent with measurements. Mugnai and Wiscombe (1980, 1989) have applied the EBCM method to axially symmetric particles with concave folds. By suitably averaging the scattering from a sphere over a small range in size parameter space to remove unrepresentative size-specific spherical resonance effects, they concluded that the sphere is probably the most anomalous scatter of all. Differences between spheres and non-spheres became significant even with a 5% deviation from sphericity. In accord with experiments, they also found that the forward scattering was reasonably well matched by a sphere, but that the side and back scattering were greatly increased over that of a single sphere. By introducing the concept of microaveraging, where the comparison is not made with a single sphere, but with the average of the scattering from many spheres with slightly different size parameters (eg., the average of

100 spheres differing by 0.01x in the size parameter from the size parameter of interest). They found that micro-averaging introduced behavior similar to that of non-sphericity, primarily by smoothing out oscillations in the phase function. However, micro-averaging alone does not reproduce either the results from experiments or from theory - shape effects are still important. The results from theoretical analysis of scattering from non-spherical particles essentially reproduces the results from experiments. However, additional effects have been noted:

i. micro-averaging always improves the agreement between spherical and non-spherical results

ii. the phase function and radiation efficiencies depend strongly on the orientation of the particle with respect to the incident radiation. Orientation averaging smooths out these variations, but caution must be applied, since even a small amount of orientation (eg, aerodynamical or magnetic) may have large effects.

iii. even small deviations from sphericity ($\approx 5\%$) can bias the non-spherical results in the same direction away from the spherical results.

iv. Q_{abs} , Q_{sca} , g, and the single particle albedo, ϖ, are not too different from those calculated by Mie theory, varying by no more than 10% (usually $< 5\%$) for $x < 20$.

Most of the systematic theoretical and experimental research has been done on compact particles. Since there is some evidence that at least a fraction of the particles in space are "fluffy" (Fraundorf, Brownlee, and Walker, 1982), the phase function and radiation efficiencies of these particles must also be studied in a systematic fashion. It is not clear that the results from compact particles will be the same for non-compact particles.

The description of non-compact, or fluffy, particles has undergone a small revolution in the last few years since the introduction of the concept of fractal (Mandelbrot, 1975, 1977, 1982). The concept of a fractal is quite simple. A fractal is a self-similar object — it appears the same regardless of the length scale used to view it. The fractal dimension of the object is a measure of the scale of repeatability. If a self-similar fractal can be covered by N replicas of itself after being reduced in size by a factor l, then the fractal dimension is $a_f = \frac{log(N)}{log(l)}$

Most particles in nature are not self similar - they do not have the same shape at all size scales. However, the particle can be described as statistically self-similar - the correlation function which describes the distribution of matter within the particle has a scale invariant form (Meakin, 1988 and references therin). For example, the mass of a fractal particle enclosed within a sphere of radius l has the form $M = l^{d_f}$. The radius of gyration R_g is a function of the mass of the particle and its distribution, and for a fractal particle, $< R_g >= M^{\frac{1}{d_f}}$. For a solid, $d_f = 3$, and the normal relationships between mass and radius are recovered.

An important property of a fractal for light scattering is its projected density (σ). This depends on the fractal dimension of the particle, and is $\sigma \propto M$ for $d_f \leq 2$ and $\sigma \propto M^{\frac{2}{d_f}}$ for $d_f \geq 2$. Additionally, the average density of the particle decreases with increasing radius: $\rho \propto l^{(D-d_f)} \propto M^{\frac{D-d_f}{D}}$, where D is the spatial dimension (usually D=3).

In practice, plots of $\log(M_p)$ versus log(size) are plotted either for a variety of different particles (each assumed to have the same fractal dimension) or for the same particle, where

the projected mass (M_p) is taken interior to the radius (Tence, Chevalier, and Julien, 1986). For fractal dimension less than 2, this yields the fractal dimension of the three dimensional particle. For fractal dimensions greater than 2, the projected image is opaque, and other methods must be used to infer the fractal dimension.

Fractal particles are important in nature, since both theory and experiment (cf Meakin, 1988 and references therein) show that when small monomers aggregate, they form fractal structures. The fractal dimension of the particle depends on the method by which the monomers aggregate: for simple ballistic aggregation, where the particles arrive as single units from infinity, $d_f \rightarrow 3$ as $l \rightarrow \infty$. If the particles coaggulate via brownian motion, $d_f = 1.7 - 1.8$. In more realistice situations, an aggregate is built up by the coaggulation of smaller aggregates, not just monomers. This process is termed cluster-cluster aggregation. Regardless of the mechanism by which the clusters are brought together (ballistically, brownian diffusion), the fractal dimension is always lower than that of an aggregate built up from monomers. For example, ballistic cluster-cluster aggregation has $d_f \approx 1.95$ (Meakin, 1988).

Other methods by which clusters are grown include re-orientation after collision (Meakin and Julien, 1985, 1988; d_f increases by 0.3 - 0.5 over aggregates without reorientation); the inclusion of van der Walls forces in the aggregation kinetics (Kennedy and Harris, 1989; $d_f \approx 2.1$, where the rate of aggregation increases by ≈ 2); and dipole interactions between particles (Mors, Botet, and Julien, 1987; d_f decreases as the strength of the dipoles increase). The review by Meakin (1988) describes in much more detail both the theoretical models and the experimental results for fractal aggregates.

The scattering from fractals has been approached from two different directions: direct calculation of the scattered intensity via the Purcell-Pennypacker method (Berry and Percival, 1986), or through the statistical scattering properties of aggregates of Rayleigh scatterers through the two-point correlation function (Martin and Hurd, 1987; Sood, 1987).

The Purcell-Pennypacker method has been described above, and has much promise in describing the scattered light from irregular particles, although research is only just beginning in this area.

The latter method relies on the fact that the scattered light from an ensemble of small ($x \ll 1$) scattering centers scales as the Fourier transform of the two-point correlation function of the ensemble. Since the two-point correlation function is a self-similar quantity ($C(r) \propto l^{-d_f}$), the scattering structure factor is also a self similar quantity: $S(q) \propto q^{-d_f}$, where q is the momentum transfer, $q = \frac{4\pi \sin(\frac{\theta}{2})}{\lambda}$, and θ is the scattering angle (Martin and Hurd, 1987). This can be rewritten in terms of the scattered intensity as

$$I \propto \frac{R^{d_f}}{q^{d_f}}$$

where R is the radius of gyration of the particle. This approximation breaks down for large and small scattering angles, where the radiation "samples" sizes larger than the radius of gyration and smaller than the smallest monomer, respectivly. The slope of the line passing through a plot of the log of the scattered intensity vs log(q) is d_f, the fractal dimension. Figure 4 shows this plot for the empirical phase function of Devine, et. al. (1986). The fractal dimension is 2.04, which suggests that the particles are almost transparent (A

particle with a fractal dimension less than 2 is "open" – chords can be found which do not intersect solid grain material) This fractal dimension is consistent with the appearance of many (but not all) of the interplanetary dust particles returned from high altitude samples of stratospheric dust (Fraundorf, Brownlee, and Walker, 1982). The fractal dimension is within the range of that found for ballistic aggregation with re-orientation (Meakin and Julien, 1988), although it is not a common dimension for aggregates without reorientation (Martin and Hurd, 1987; Meakin, 1988). Note however, that the basic premise upon which statistical properties of the light scattering is founded ($x \ll 1$ for the smallest monomers) may not hold for IDP – type particles, since many of these have monomer units of $\approx 1\mu m$ (Fraundorf, Brownlee, and Walker, 1982).

Future work should focus on the optical properties of fractal particles as a function of fractal dimension and composition. Since most IDP are inhomogeneous, the scattering properties of inhomogeneous particles should also be investigated, and compared with effective medium theories. Additionally, theoretical work needs to be done with respect to the formation and destruction mechanism of fractal particles in comets. An important, but somewhat neglected aspect of shape effects is the effect on the spectral signature near strong absorption peaks (BH contain a good description of the effects of shape on the spectrum). Referring back to Figure 2, spheres will absorb most strongly where $\epsilon' = -2$. Discs and needles have two absorption peaks, the strongest where ϵ'' peaks. Ellipsoids will have three peaks, and a cumulative distribution of ellipsoids (BH) will have a very wide, and slightly asymmetrical absorption peak. This phenomena has been applied to understanding the 11.3 μm crystalline silicate feature in P/Halley and C/Bradfield (Lien and Hanner, 1989).

V Applications to Cometary Dust

The dust coma of a comet is composed of dust ejected from active regions on the nucleus in directions which depend on the specifics of the rotation of the comet. A single dust grain is probably heterogeneous in composition and non-spherical in shape. The ejection velocity from the nucleus is a function of size, shape, and composition, thus the particle size distribution in the coma will be a function of radial and azimuthal positions. Grain fragmentation or aggregation may occur, changing the local size distribution. Furthermore, the particle size distribution at any point may be different for different grain types (eg., CHON, silicates, etc.). Our problem is the inverse: given observations of the coma projected onto the plane of the sky, we wish to ascertain the cometographic positions of the dust jets, the composition and particle size distribution of the dust at the surface, ejection velocities and times, and particle shapes. Although this task seems rather formidable, a great deal of progress has been made in the past few years.

In this section, a brief review of the application of optical constants and scattering theory toward the interpretation of cometary observations is presented. The application of optical constants and scattering theories toward comets falls into five areas: polarization, scattering, kinematics, thermal emission, and theoretical investigations.

The polarization of cometary dust is indicative of the shape, size, and complex index of refraction. Polarization studies of comets show that the all behave qualitatively in the same way: a small negative polarization for phase angles $\leq 20°$; neutral polarization around $20° - 22°$, and a linear rise in the polarization at larger phase angles. (Isobe et al., 1978; Dolfus and Suchail, 1987; Dolfus et al., 1988; Kikuchi et al, 1987; Brooke, Knacke, and Joyce, 1987)). A slight increase in polarization with wavelength has also been noted ($\approx 50\%$ over $\Delta\lambda \approx 1\mu m$; Dolfus et al, 1988; Kikuchi et al., 1987).

To interpret the polarization, Mie theory has been used almost exclusively. The basic technique is to calculate the polarization as a function of phase angle for a grid of real and imaginary indices of refraction with an assumed form of the particle size distribution, and then find the "best fit" (usually in a least-squares sense) to the observations. Myers (1985) could not find an acceptable fit to the observations for the particle size distributions he used. Brooke, Knacke, and Joyce (1987) used the particle size distribution derived from the Vega SP-2 detector, and also concluded that a single index of refraction fit cannot reproduce the observations. They introduced a two component model, and found a good fit for m = 1.7 +i0.3 for the first component, and m = 1.4+i0.05 for the second, where the first is 3.5 times more abundant that the second. Mukai, Mukai, and Kikuchi (1987) found that their data could be fit with the Vega particle size distribution for an index of refraction of m = 1.39+i0.024. They did not need a second component. Note that the real index of refraction of 1.4 is very close to the lower limit for terrestrial silicates (Egan and Hilgeman, 1979), although the derived imaginary index is over an order of magnitude larger. The derived index of refraction is also similar to the complex index of refraction of dirty ice (Lien, 1990).

Perrin and Lamy (1983) have shown theoretically that the polarization from *single* rough grains can reproduce the general trends observed in comets, the zodiacal light, and labratory measurements of rough particles. Zerull (1976) also shows experimentally that the same trends as observed in comets are also observed in irregular particles, although his angular sampling interval is not as high as those made for comets. Clearly, care must be taken in interpreting the derived optical constants until the effects of roughness on polarization are more clearly understood.

A final note of caution should be made concerning measurements of polarization with variable size apertures. Eaton, Scarrott, and Warren-Smith (1988) show that the maximum polarization occurs in dust jets which are not symmetric with respect to the center of brightness. The polarization adduced from aperture photopolarimetry may depend strongly on the aperture size and placement.

Most of the comparisons with scattered solar radiation and scattering theories has been accomplished with Mie theory (cf Hanner, 1980 and Campins and Hanner, 1982 for recent reviews). The scattered radiation from cometary dust tends to be somewhat red, with a slope of 5 - 10% per 1000 Å (A'Hearn, 1982; Remillard and Jewitt, 1985; Jewitt and Meech, 1986). There may be a change in the slope as a function of wavelength, however, going from red in the visible to blue in the near IR (Meech, 1988), as well as a change in the color with heliocentric distance (Hartmann and Cruikshank, 1984).

The phase function of the dust is the very difficult to obtain, since the the physical conditions within the coma are very different as the comet-earth angle changes with time.

In spite of the difficulty of the measurment, Ney and Merrill (1976) managed to obtain an approximate phase function for comet West. This phase function has been used extensively for modelling cometary dust (Divine et al., 1986). Qualitatively, the phase function shows the strong forward scattering lobe for angles less than $\sim 30°$, a relatively flat response for intermediate angles, and a small increase for angles $\geq 140°$. There does not appear to be a strong backscattering peak near 180° (Meech and Jewitt, 1987), however, only recently has the strong backscattering peak for satellite surfaces been seen (Dominque et al., 1989) and it is found to be exceedingly narrow $\leq 0.5°$). Recent searches for the backscattering phenomena in P/Halley (Meech and Jewitt, 1987) only go as low as 1.37°.

Application of Mie theory to the scattering phenomena (Campins and Hanner, 1982; Remillard and Jewitt, 1985) indicate that spheres larger than $2\mu m$ with optical constants similar to those found in terrestrial silicates are needed to explain the general charactersitics of the color and phase function. Unfortunately, the phase function and color are not very sensitive to either size or composition for $x \geq 1 - 5$.

The largest difficulty with the application of Mie theory to the problem of scattering from cometary grains is the difficulty of Mie theory to reproduce the large side scattering cross section of rough grains (cf section IV). Clearly, much more work needs to be done in interpretting the scattering from cometary dust in terms of irregular particles.

Because of the difficulty in applying directly Mie theory to the scattered light from comets, most published continuum photometry parameterizes the scattering in terms the of the average albedo and the average cross section for scattering. Perhaps the most extensive work has been done by A'Hearn and co-workers (A'Hearn and Millis, 1980; A'Hearn, et al., 1984; Schleicher et al., 1989), where they parameterize the continuum scattering by the quantity $AF\rho$, where A is the albedo, f is the filling factor ($f = \frac{N\sigma}{\pi\rho^2}$), ρ is the radius of the aperture, σ is the average grain cross section (equivalent to $C_{sca}P(\theta)$), and N is the total number of grains within the aperture. If the projected density of the dust decreases as ρ^{-1}, then the quantity $Af\rho$ is determined from directly measurable quantities and is independent of the geocentric distance or the aperture size (A'Hearn, et al., 1984).

An interesting, and as yet untapped, property of scattering is the sensitivity of the forward scattering lobe to the size distribution. Hodkinson (1966) has pointed out that for $x \geq 1$, the forward scattering lobe ($0° - 20°$) depends almost solely on the particle size distribution, with only a minor dependence on the composition. This observation could be made by an instrument such as the Solar Maximum Mission. An alternate method is to use the profile of a star during an appulse. There should be a significant change in the profile due to the forward scattering properties of the dust. The magnitude of the change will depend on the amount of dust along the line of sight. The detection of a slight decrease in the amount of light from a star during an appulse by C/IRAS-Aracki-Alcock (Lecacheux et al., 1984) suggests that such an observation may be feasible.

The kinematics of dust tails has been understood since the time of Bessel, and with modifications by Bredichin, quantitative analysis was able to be undertaken (Bobrovnikoff, 1929). Once ejected from the nucleus, the dust particle is subject only to the attractive force of gravit from the sun, and the repulsive force due to radiation pressure (Lorentz forces are assumed to be negligible for particles responsible for the scattered solar continuum). The ratio of the repulsive radiation force to the force of gravity can be expressed as

$\beta = \frac{F_r}{F_g} = 1.19 \times 10^{-4} \frac{Q_{pr}}{\rho d}$, where ρ is the density and d is the diameter of the dust grain (cgs units; Finson and Probstein, 1968). The radiation pressure efficiency, Q_{pr} , is related to the size of the particle and the optical constants through scattering theory (Bohren and Huffman, 1983). Burns, Lamy, and Soter (1979) have calculated Q_{pr} for a variety of different materials. The maximum of Q_{pr} occurs for particles $\approx 0.1 - 1.0\mu m$ in radius. For smaller radii, Q_{pr} decreases faster than d^{-1}, causing a net decrease in Q_{pr} . As $Q_{pr} \rightarrow 1 - 2$, $\beta \propto d^{-1}$. Note that since the density of the dust is thought to be size dependent (Divine, et al., 1986), the maximum of β will depend on the form of the density - radius relationship. Little work has been done theoretically or experimentally to determine the effects of particle roughness or porosity on Qpr.

The kinematics of the dust tail depends on β and the ejection velocity (Finson and Probstein, 1968; Kimura and Liu, 1977; Fulle, 1987). The result of modelling the observed dust tail is a β-distribution instead of a size distribution. To convert to a size distribution the relationship between β and radius is needed. To determine absolute number of dust particles, the scattering properties of the dust must also be known. If the dust is irregular and porous, then assuming the particles are spheres of a given composition will cause a shift in the size distribution toward smaller particles, but an increase in the total number of particles. Theoretical work on the effects of non-sphericity and porosity will help determine the magnitude of these errors.

An interesting conclusion from observations of dust tails is the predominance of $1 - 10\mu m$ grains in the dust tails (Finson and Probstein, 1968b; Sekanina and Miller, 1973; Sekanina and Schuster, 1978a, 1978b; Kimura and Liu, 1977; Fulle, 1987; Fulle, 1989). Since these grains are the same size as those responsible for the normal coma (cf above and discussion of thermal radiation below), then an interesting, and currently unanswered question is: where are the visible dust tails for most comets? For example, C/IRAS-Araki-Alcock did not show a discernable visible dust tail, but had an extensive dust tail as determined from thermal IR measurments (Walker, et al., 1984).

A unique application of the kinematical theory of dust tails has recently been applied to the analysis of the dust *trail* of P/Tempel 2 (Sykes, Lien, and Walker, 1989). They showed that the dust trail of P/Temple 2 detected by IRAS could be explained by low β dust ($\beta \leq 10^{-3}$) ejected at very low velocities ($\leq 10m/s$) over many (≥ 10) orbital periods. The low values for both the expansion velocity and β suggest centimeter or larger size particles.

A great deal of effort is currently being applied toward the analysis of the dust tails of comets. Proper interpretation of the results of these analyses awaits the results from theoretical and experimental research on the effects of composition, non-sphericity, and porosity on Q_{pr} .

The application of scattering theories toward the understanding of cometary dust has been most successful in the analysis of the thermal IR (Hanner, 1980; Campins and Hanner, 1982; Eaton, 1984; Lien, 1990). A fraction of the solar radiation incident upon a dust grain is absorbed, then re-emitted in the thermal IR. In general, the $8 - 13\mu m$ region can be fit by a single blackbody, approximately 10-15% hotter than a blackbody at the heliocentric distance of the observation. This increase of the effective temperature is consistent with observations out to $100\mu m$ (Herter, Campins, and Gull, 1987; Glaccum,

et al., 1987), although the amount of the excess temperature may depend on the spectral region observed.

For many comets, a broad emission feature at centered at $10\mu m$ is observed when the comet is within ≈ 1 AU of the sun, although this limit is quite variable (cf Ney, 1982). Indeed, some comets never show the emission feature. This feature has been identified as arising from an amorphous silicate, and must be due to grains smaller than about 5 μm (Hanner, et al., 1987 and references therein).

Recently, a new spectal feature at $11.3\mu m$ has been observed in two comets, P/Halley (Bregman et al, 1987, Combes et al, 1988, Campins and Ryan, 1989) and C/Bradfield (Hanner et al, 1989), and has been attributed to a component of crystaline olivene in the dust. Lien and Hanner (1989) have shown that the crystalline silicate component is probably 25-50% of the total silicate abundance.

The equilibrium temperature of a small grain (assumed isothermal) in space depends on its size, composition, and shape (Lamy, 1974; Mukai, 1977; Campins and Hanner, 1982; Lamy, 1988; Lien, 1990). At 1 AU, small spherical grains which are even slightly absorbing at optical wavelengths are very hot (350 K - 600K). The equilibrium temperature drops below that of a blackbody for grains between $0.1 - 1.0\mu m$, then slowly approaches the temperature of a blackbody as the radius increases. For slightly rough particles with radii between $10\mu m$ and $100\mu m$ the equilibrium temperature is above that of a blackbody, then slowly decrease to the blackbody temperature as the particle size increases past $100\mu m$ (Lamy, 1988). The observed excess in the thermal flux over that of a blackbody at the same heliocentric distance is thus thought to be due to non-spherical effects. More theoretical research needs to be done with respect to the effects of non-sphericity on the equilibrium grain temperature.

The shape and strength of the 10 μm silicate feature is evidence for the existence of small ($\leq 1\mu m$) grains (Hanner et al., 1987). Along with the contribution of the large grains to the background thermal emission, the particle size distribution and the relative abundances of the silicates can be determined from the observations, although usually the form of the particle size distribution is assumed and the relative abundances of the components are determined (Hanner, 1980; Campins and Hanner, 1982). The thermal IR flux from P/Halley has also been shown to be consistent with the particle size distribution derived from *in situ* measurements (Hanner, et al., 1987; Herter, Campins, and Gull, 1987; Glaccum, et al., 1987).

Usually the calculations are done using the optical constants of homogeneous minerals (cf Table I for a list of optical constants currently in use by most cometary researchers). An interesting comparison with the thermal spectrum of P/Halley with the predicted flux from Mie theory using optical constants derived from a polished slab of lunar basalt has been presented (Krishna Swamy, et al., 1988). Although they were able to fit the observed spectrum reasonably well, the interpretation of the results in terms of total abundance of silicates, absorbing material, etc, is not clear due to the heterogeneity of the material from which the optical constants were derived.

The current difficulty with the Mie theory appears to be the inability of spherical particles to predict the excess in the equilibrium temperature over that of a blackbody. Mie theory almost always predicts an equilibrium temperature lower than that of an equivalent

blackbody radiator for $1 < x < 100$. Non-spherical effects may provide the answer, but the interpretation of Q_{abs} may not be simple. For example, Q_{abs} for a 2:1:1 spheroid can change by more than a factor of 2 depending on the size parameter and index of refraction (Lien and Hanner, 1989). The "equilibrium temeprature" will depend on the orientation of the particle with respect to the incident radiation. If the particle is rapidly spinning, there will be an '"effective *Qabs*." It is not clear if this is equivalent to an orientation-averaged Q_{abs} . Additionally, since polarization maps of P/Halley (Eaton, Scarrott, and Warren-Smith, 1988) show that the jets are more polarized than the surrounding com, suggesting partial alignment of the grains — orientation averaging Q_{abs} may not be an appropriate procedure in these situations. Clearly, more work needs to be done to understand the effects of non-sphericity on the equilibrium grain temperature.

Other purely theoretical investigations applying scattering theories toward cometary dust should also be mentioned. The first is the determination of the lifetime of ice grains, both pure and "dirty ice." This question was first broached by Hanner (1982) for pure ice and "dirty ice" defined as pure ice with a non-zero imaginary component at optical frequencies. The use of effective medium theories has been applied to this problem by Mukai (1986), Mukai, et al. (1986), Mukai, Mukai, and Kikuchi (1989), and Lien (1990). The conclusion reached is that with even a small amount of "dirt ($\leq$ 1%), icy grains sublimate very rapidly. As they sublimate, they become "dirtier" if the "dirt" is the matrix, or break into smaller, probably dirty, ice grains, which sublimate even more quickly. For example, a 100 μm grain with 1% of the volume filled with magnetite will sublimate away in less than 1000 s at 1 AU, assuming that the volume fraction of magnetite remains constant (Lien, 1990).

The second theoretical investigation concerns the effects of heterogeneity on the thermal spectrum and equilibrium temperature of cometary dust. Since not a single homogeneous interplanetary dust particle has ever been observed, there is no reason to believe that cometary dust is homogeneous. Using effective medium theories (cf section III), Lien (1990) showed that the equilibrium temeprature for small grains is very sensitive to the composition for a mix of magnetite (a typical absorbing material) and amorphous silicate. The spectrum showed the 10 μm silicate feature for fractional abundances of amorphous silicate greater than about 10%. For grains larger than $\approx 5\mu m$, the equilibrium grain temperature was almost independent of composition ($\approx$ 10% variations), and the thermal spectrum was essentially featureless. The same methodology was applied toward understanding the conditions under which a heterogeneous grain composed of both crystalline and amorphous silicate would show the 11.3 μm feature of crystalline olivene (Lien and Hanner, 1989). It was concluded that the observations were consistent with a volume fraction of crystalline olivene of between 10% and 50%.

Finally, investigations have begun on the effects of non-sphericity. Currently, research has been reported on the thermal/scattering properties of irregular particles (Perrin and Lamy, 1986; Lamy, 1988) and on the effects of non-sphericity on the wavelength shift of narrow spectral features (Lien and Hanner, 1989). To reiterate, Perrin and Lamy (1986) found, consistent with laboratory experiments, that the scattered flux and polarization from rough particles is inconsistent with equivalent volume spheres. Lamy (1988) has begun to apply the results toward the equilibrium grain temperatures of rough grains, and

finds that Mie theory is adequate in its predictions for most sizes, but that rough particles are predicted to have much larger equilibrium temperature for particle radii between 10 μm and 100 μm. Lien and Hanner (1989) showed that there is a significant shift in the wavelength of the peak of the crystalline olivene emission feature from 11 μm to 11.3 - 11.4 μm due to non-sphericity effects, consistent with observations.

An important question when interpreting observations using scattering theories is: to what extent is the solution unique? For example, the determination of the particle size distribution is closely coupled with the determination of the composition. Each particle of a single size and composition in the cometary coma has a unique spectral signature. By attempting to approximate this signature with an assumed composition and set of optical properties (usually derived from Mie theory), the spectrum of the comet is inverted to determine the number of particles of each size. Since particles of slightly different sizes and compositions have almost identical spectral signatures, there are limits on the precision of the inversion (cf Heintzenberg and Welch, 1982, Heintzenberg and Baker, 1976, Holland and Gagne, 1970, Holland and Draper, 1967, and Capps and Hess, 1984) for descriptions of the inverse problem for scattered radiation, and Crifo, 1987, 1988 for a description of its application to the inversion of the IR spectrum). In most cases, the form of the size distribution is assumed, and the variables optimized to reproduce the observed spectrum with the assumed composition. This may lead to erroneous conclusions if a) the form of the particle size distribution is not close to the "real" size distribution; b) the composition of the grains is incorrectly guessed; c) the wrong optical constants are used to approximate the assumed composition; or d) the wrong theory is used to determine the optical signatures of the grains.

Crifio (1988a, 1988b) discusses some of these problems as applied to cometary dust by comparing optical and infrared observations with those calculated from Vega - or Giotto - derived particle size distributions and realistic optical constants, along with a theoretical treatment of the dynamics of the ejected dust. He finds, similar to others, that the optical scattering and thermal IR fluxes cannot simultaneously be explained within a factor of 2 using Mie theory. However, if only the IR data are used, agreement can be reached between observation and theory. Crifio also points out that the form of the particle size distribution chosen can significantly alter the conclusions - for example, previous particle size distributions underestimated both the high and low mass ends of the *in situ* dust fluence. Thermal IR fluxes calculated using the *in situ* particle size distributions can reproduce the observations, but the result is a significantly larger dust to gas ratio (≥ 1) and most of the mass is in the large grains (Crifio, 1988b).

Numerical experiments such as those by Crifio (1988a, 1988b) are very important in understanding the sensitivity of the observations to various physical parameters. However, further work is needed to assess the effects of non-sphericity, porosity, time- and spatial- dependence of dust emission, and composition heterogeneity on the thermal and scattered flux. By comparing the results with observations, the physical limits on each of the parameters can be determined.

V Summary

The focus of this review has been on the application of measured optical constants toward the interaction of electromagnetic radiation with small particles, with an emphasis on the interpretation of cometary observations. With this in mind, a number of conclusions and recommendations can be made concerning the interpretation of cometary dust.

1) Optical constants are not constant. In some spectral regions, the optical constants vary rapidly with wavelength. Thus, one should be wary of "average optical constants" – optical constants which have been derived as "representative" of the average bulk properties of the constituent material. These average optical constants are usually derived by assuming a single characteristic particle size and finding the optical constant which, when applied with the Mie theory, best represents the observations. In most cases, the derived optical constants are not representative of naturally occuring materials (see Bohren and Huffman, 1983 for a good discussion of this).

2) The optical constants may be incorrect. Because of errors in measurement, or the application of the Kramers-Kronig relationship over too small a spectral region, or an improperly pressed powdered sample, the derived optical constants may be in error. A full Kramers–Kronig analysis and application of the more important sum rules should be performed on any set of optical constants whose accuracy is important.

3) Optical constants derived from the measurement of inhomogeneous materials, where the inhomogeneities are of comparable size to the size of the beam of radiation used in the experiment should not be used to predict the optical properties of small particles. Clearly, the optical constants will vary as a function of position on the sample; hence what is the meaning of the comparison between the theory and the observation?

4) Effective medium theories appear to be powerful tools in understanding the effects of heterogeneity upon the spectrum from an ensemble of small particles. The results from comparisons with data should be used to induce a laboratory to measure the optical constants of the optimal mixture. Also note the limitations of these theories – they all assume that the particles are very small compared with the wavelength of the incident radiation.

5) Mie theory is the predominant theory used to describe the interaction of radiation with small particles. However, this theory has severe limitations in describing certain effects. For example, irregular particles scatter light in the side and backward directions much more efficiently than can be accounted for by Mie theory. The observation that cometary dust is very dark is also inexplicable by Mie theory – particle size distributions which match the thermal IR flux always overestimates the amount of scattered light in the visible by factors of 2 – 10 (Crifio, 1988a, 1988b). Mie theory also predicts equilibrium grain temperatures which are a 5K – 30K cooler than observed.

6) New numerical methods have been developed to calculate the optical properties of non-spherical particles (EBCM, Purcell-Pennypacker method, etc). In addition, new statistical methods have been developed to describe irregular particles (fractals). A union of these methods may be the most appropriate way to deal with the observations and analysis of cometary dust.

7) The inverse problem - determining the composition and particle size distribution from observations - does not have a unique solution. However, the solution can be constrained by utilizing different sets of observations: polarization, scattering, thermal, *in*

situ measurments (which can only be used for the line of sight along the trajectory of the spacecraft), and theoretical modelling of the gas and dust dynamics. Investigations into the sensitivity of the inversion to the various parameters can help in structuring observing programs to optimize the inversion.

The author wishes to express his thanks to M. Sykes and M. Hanner for interesting discussions, and especially to R. Newburn for providing the opportunity for this work to be included in this volume. This work was supported in part by Air Force Geophysics Lab contract number F19628-87-K-0045.

References

A'Hearn, M. F., 1982. *Comets*, ed. L.L. Wilkening, University of Arizona Press, Tucson, p. 433.

A'Hearn, M. F. and Millis, R., 1980. Astron. J. /bf 85, 1528.

A'Hearn, M.F., Schleicher, D., Feldman, P., Millis, R., and Thompson, D., 1984. Astron. J. **89**, 579.

Asano, S. and Yamamoto, G., 1975. Appl. Opt. **14**, 962.

Aspnes, D.E., 1985. In *Handbook of Optical Constants of Solids*, E.D. Palik, ed. p. 89.

Barber, P. and Yeh, C., 1975. Appl. Opt. **14**, 2864.

Bell, E.E., 1967. In *Handbuch der Physik*, v 25, 2a, p. 1. Ed. S. Fl ü gge, Springer-Verlag, New York.

Bell, R.J., Ordal, M.A., and Alexander, R.W., 1985. Appl. Opt., **24**, 3680.

Berry, M.V. and Percival, I.C., 1986. Optica Acta **33**, 577.

Bobrovnokoff, N.T., 1929. Publ. Astron. Soc. Pacific **40**, 164.

Bohren, C.F., 1986. J. Atmos. Sci. **43**, 468.

Bohren, C.F. and Battan, L.J., 1980. J. Atmos. Sci. **37**, 1821.

Bohren, C.F. and Huffman, D.R., 1983. *Absorption and Scattering of Light by Small Particles*, Wiley-Interscience, New York. (BH)

Bohren, C.F. and Nevitt, T.J., 1983. Appl. Opt. **22**, 774.

Bregman, J.D., et. al, 1987. Astron. Astrophys. **187**, 616.

Brooke, T.Y., Knacke, R.F., and Joyce, R.R., 1987. Astron. Astrophys. **187**, 621.

Bruggeman, D.A.G., 1935. Ann. Phys. (Leipzig), **24**, 636.

Burns, J.A., Lamy, P.L., and Soter, S., 1979. Icarus **55**, 1.

Campins, H. and Hanner, M., 1982. In *Comets*, L.L. Wilkening, (Ed.), University of Arizona Press, Tucson, p. 341.

Campins, H. and Ryan, E.V., 1989. Ap. J. **341**, 1059.

Capps, C.D., and Hess, G.K., 1984. In *Proceedings of the 1984 CSL Conference on Obscuration and Aerosol Research*, R.E Kohl, ed., p. 139.

Coletti, A., 1984. Aerosol Sci. Tech. **3**, 39.

Combes, M., Lecacheux, J., Encrenaz, T., Sicardy, B., and Zeau, Y., 1983. Icarus **56**, 229.

Crifo, J.F., 1988a. Proc Xth European Regional Astronomy meeting of the IAU, Tchecoslovac Academy af Sciences.

Crifo, J.F., 1988b. Part. Part. Syst. Charact. **5**, 38.

Deirmendjian, D., 1969. *Electromagnetic Scattering on Spherical Polydispersions*, Elsevier, New York.

Divine, N., et. al, 1986. Space Sci. Rev. **43**,1.

Dolfus, A., 1989. Astron. Astrophys. **213**, 469.

Dolfus, A. and Suchail, J.-L., 1987. Astron. Astrophys. **187**, 669.

Dolfus, A., Bastien, P., LeBorgne, P., Levasseur-Regourd, J.-F., and Mukai, T., 1988. Astron. Astrophys. **206**, 348.

Domingue, D., Hapke, B., Lockwood, W., and Thompson, D., 1989. B.A.A.S. **21**, 984.

Draine, B.T., 1988. Ap. J. **333**, 848.

Drolen, B.L., and Tien, C.L., 1987. J. Quant. Spectrosc. Radiat. Transfer **37**, 433.

Eaton, N., 1984. Vistas in Astr., **27**, 111.

Eaton, N., Scarrott, S.M., and Warren-Smith, R.F., 1988. *Infrared Observations of Comets Halley and Wilson and Properties of the Grains*, M.S. Hanner, ed. NASA CP3004, p. 139.

Edoh, O., 1983. Ph.D. Thesis, University of Arizona.

Egan, W.G. and Hilgeman, T.W., 1979. *Optical Properties of Inhomogenous Materials. Applications to Geology, Astronomy, Chemistry, and Engineering*, Academic, New York.

Finson, M.L. and Probstein, R.F., 1968a. Ap. J. **154**, 327.

Finson, M.L. and Probstein, R.F., 1968b. Ap. J. **154**, 353.

Fraundorf, P., Brownlee, D.E., and Walker, R.M., 1982. In *Comets*, L.L Wilkening (Ed), University of Arizona Press, Tucson, p. 383.

Fulle, M., 1987. Astron. Astrophys. **171**, 327.

Fulle, M., 1989. Astron. Astrophys. **217**, 283.

Gallily, I., 1985. In *Proceedings of the 1984 CSL Conference on Obscuration and Aerosol Research*, R.E Kohl, ed., p. 115.

Gerber, H.E. and Hindeman, E.E., eds., 1980. *Light Absorption by Aerosol Particles*, Spectrum, Hampton.

Gillespie, J.B. and Goedecke, G.H., 1989. Appl. Opt. **28**, 3985.

Glaccum, W., Moseley, S.H., Campins, H., and Loewenstein, R.F., 1987. Astron. Astrophys. **187**, 635.

Hanner, M. S., 1980. *Solid Particles in the Solar System*, eds. I. Halliday and B. McIntosh, Dordrecht, D. Reidel, p. 223.

Hanner, M.S., Giese, R.S., Weiss, K., and Zerull, R., 1981. Astron. Astrophys. **104**, 42.

Hanner, M.S., Tokunaga, A.T., Golisch, W.F., Griep, D.M., and Kaminski, C.D., 1987. Astron. Astrophys. **187**, 653.

Goedecke, G.H., and O'Brien, S.G., 1988. Apl. Opt. **27**, 2431.
1981. Astron. Astrophys. **104**, 42.

Hansen, J.E. and Travis, L.D., 1974. Space Sci. Rev. **16**, 527.

Hartmann, W.K., and Cruikshank, D.P., 1984. Icarus **57**, 55.

Heintzenberg, J. and Baker, M., 1976. Appl. Opt. **15**, 1178.

Heintzenberg, J. and Welch, R.M., 1982. Appl. Opt. **21**, 822.

Herter, T., Campins, H., and Gull, G.E., 1987. Astron. Astrophys. **187**, 629.

Hodkinson, J.R., 1966. Appl. Optics **5**, 839.

Holland, A.C. and Draper, J.S., 1967. Appl. Opt. **6**, 511.

Holland, A. C. and Gagne, G., 1970. Appl. Opt. **9**, 1113.

Huffman, D.R., 1975. Astrophys. Space Sci., **34**, 175.

Huffman, D.R., 1977. Adv. in Physics, **26**, 129.

Huffman, D.R., 1989. In *Optical Effects Associated with Small Particles*, P.W. Barber and R.K. Chang, eds., World Scientific, , New Jersey, p. 279.

Huffman, D.R. and Stapp, J.L., 1973. IAU Symp. 52 Interstellar Dust and Related Topics, p. 297.

Hunter, W.R., 1985. In *Handbook of Optical Constants of Solids*, E.D. Palik, ed. p. 69.

Iskander, M.F., Chen, H.Y, and Penner, J.E., 1989. Appl. Opt. **28**, 3083.

Iskander, M.F., Lakhtakia, A., and Durney, C.H., 1983. IEEE Trans. Antennas Propag. **AP-31**, 317.

Isobe, S., Saito, K., Tomita, K., and Maehara, H., 1978. Publ. Ast. Soc. Japan **30**, 687.

Jensen, B., 1985. In *Handbook of Optical Constants of Solids*, E.D. Palik, ed. p. 169.

Jewitt, D. and Meech, K., 1986. Astrophys. J. **310**, 937.

Kattawar, G.W., and Humphreys, T.J., 1980. In *Light Scattering by Irregularly Shaped Particles*, D. Schuerman, (Ed.), Plenum, New York, p. 177.

Kennedy, I.M. and Harris, S.J., 1989. J. Colloid Interface Sci. **130**, 489.

Kerker, M.,1969. *The Scattering of Light and Other Electromagnetic Radiation*, Academic, New York.

Kerker, M., Scheiner, P., and Cooke, D.D., 1978, J. Opt. Soc. Am. **68**, 135.

Khare, B.N., Sagan, C., Arakawa, E.T., Suits, F., Callcott, T.A., and Williams, M.W., 1984. Icarus **60**, 127.

Khare, B.N., Sagan, C., Thompson, W.R., Arakawa, E.T., and Votaw, P., 1987. J. Geophys. Res. **92**, 15,067.

Kikuchi, S., Mikami, Y., Mukai, T., Mukai, S., and Hough, J,H., 1987. Astron. Astrophys. **187**, 689.

Kimura, H. and Liu, C.-P., 1977. Chin. Astr. **1**, 235.

Koike, C., Hasegawa, H., Asada, N., and Komatuzaki, T., 1989. Mon. Not. R. astr. Soc. **239**, 127.

Krishna Swamy, K.S., Sanford, S.A., Allamandola, L.J., Witteborn, F.C., and Bregman, J.D., 1988. Icarus, **75**, 351.

Lamy, P.L., 1974. Astron. Astrophys. **35**, 197.

Lamy, P. 1988. *Infrared Observations of Comets Halley and Wilson and Properties of the Grains*, M.S. Hanner, ed. NASA CP3004, p. 29.

Lamy, P.L. and Perrin, J., 1988. Icarus **76**,100.

Lien, D.J., 1990, Ap. J., in press.

Lien, D.J. and Hanner, M.S., 1989. B.A.A.S. **21**, 940.

Mandelbrot, B.B., 1975. *Les Objets Fractals: Forme et Dimension*, Flammarion, Paris.

Mandelbrot, B.B., 1977. *Fractals: Form, Chance, and Dimension*, W.H. Freeman, San Francisco.

Mandelbrot, B.B., 1982. *The Fractal Geometry of Nature*, W.H. Freeman, New York.

Martin, J.E. and Hurd, A.J., 1987. J. Appl Cryst, **20**, 61.

Maxwell-Garnett, J.C., 1904. Phil. Trans R. Soc. **A203**, 385.

Meakin, P., 1988. Adv. Colloid and Interface Science, **28**, 249.

Meakin, P. and Julien, R., 1985. J. Physique. **46**, 1543.

Meakin, P. and Julien, R., 1988. J. Chem Phys. **89**, 246

Meech, K., 1988. *Infrared Observations of Comets Halley and Wilson and Properties of the Grains*, ed. M.S. Hanner, NASA CP3004, p. 172.

Meech, K. and Jewitt, D., 1987. Astron. Astrophys. **187**, 585.

Mors, P.M., Botet, R., and Julien, R., 1987. J. Phys A. **20**, L975.

Mugnai, A. and Wiscombe, W.J., 1980. J. Atmos. Sci. **37**, 1291.

Mugnai, A. and Wiscombe, W.J., 1989. Appl. Opt. **28**, 3061.

Mukai, T., 1977. Astrophys. Space Sci. **51**, 165.

Mukai, T. 1986. Astron. Astrophys. **153**, 213.

Mukai, T., Fechtig, H., Grun, E., Giese, R.H., and Mukai, S., 1986. Astron. Astrophys. **167**, 364.

Mukai, T. and Koike, C., 1989. Preprint.

Mukai, T., Mukai, S., and Kukuchi, A., 1987. Astron. Astrophys. **187**, 650.

Myers, R.V., 1985. Icarus **63**, 206.

Ney, E.P., 1982. In *Comets*, L.L. Wilkening, (Ed.), University of Arizona Press, Tucson, p. 323.

Ney, E.P. and Merrill,, K.M., 1976. Science **194**, 1051.

Nussenzveig, H.M. and Wiscombe, W.J., 1980. Phys. Rev. Letters **45**, 1490.

Ostro, S.J., 1987. Astron. Astrophys. **176**, 358.

Palik, E.D., 1985 (ed.). *Handbook of Optical Constants of Solids*, Academic Press, New York.

Perrin, J.M. and Chiappetta, P., 1985. Optica Acta. **32**, 907.

Perrin, J.M. and Lamy, P.L., 1986. Optica Acta, **33**, 1001.

Pollack, J.B. and Cuzzi, J.N., 1980. J. Atmos. Sci. **37**, 868.

Potter, R.F., 1985. In *Handbook of Optical Constants of Solids*, E.D. Palik, ed. p. 11.

Purcell, E.M. and Pennypacker, C.R., 1973. Ap. J. **186**, 705.

Querry, M., 1984. In *Proceedings of the 1984 CSL Conference on Obscuration and Aerosol Research*, R.E Kohl, ed., p. 147.

Querry, M., 1985. In *Proceedings of the 1984 CSL Conference on Obscuration and Aerosol Research*, R.E Kohl, ed., p. 145.

Querry, M., 1986. In *Proceedings of the 1984 CSL Conference on Obscuration and Aerosol Research*, R.E Kohl, ed., p. 163.

Remillard, R.P. and Jewitt, D.C., 1985. Icarus, **64**, 27.

Schleusner, S.A., Lindberg, J.D., and White, K.O., 1975. Appl. Opt. **15**, 2564.

Schleicher, D., Millis, R.L., Osip, D.J., A'Hearn, M.F., and Birch, P.V., 1989. B.A.A.S. **21**, 936.

Schuerman, D. (Ed.), 1980. *Light Scattering by Irregularly Shaped Particles*, Plenum, New York.

Schuerman, D., Wang, R., Gustafson, B, and Schaefer, R., 1981. Appl. Opt. **20**, 4039.

Sekanina, Z. and Farrell, J.A., 1980. Astron. J. **85**, 1538.

Sekanina, Z., Larson, S.M., Emerson, G., Helin, E.F., and Schmidt, R.E., 1987. Astron. Astrophys. **187**, 645.

Sekanina, Z. and Miller, F.D., 1973. Science **179**, 565.

Sekanina, Z. and Schuster, A.E., 1978a. Astron. Astrophys. **65**, 29.

Sekanina, Z. and Schuster, A.E., 1978b. Astron. Astrophys. **68**, 429.

Singham, S.B. and Bohren, C.F., 1989. Appl. Opt. **28**, 517.

Smith, D.Y., 1985. In *Handbook of Optical Constants of Solids*, E.D. Palik, ed. p. 35.

Sood, A.K., 1987. Hyperfine Int. **37**, 365.

Steyer, T.R., 1974. Ph.D. Thesis, University of Arizona.

Sykes, M., Lien, D.J., and Walker, R.G., 1989. Icarus, submitted.

Tence, M., Chevalier, J.P., and Julien, R., 1986. J. Physique **47**, 1989.

Toon, O.B., Pollack, J.B., and Khare, B.N., 1976. J. Geophys. Res. **81**, 5733.

Ungat, A., Grehan, G., and Gouesbat, G., 1981. Appl. Opt. **20**, 2911.

van de Hulst, H.C, 1957. *Light Scattering by Small Particles*, Dover, New York.

Voltz, F.E., 1972. Appl. Opt. **11**, 755.

Walker, R.G., Aumann, H.H., Davies, J., Green, S., de Jong, T., Houck, J.R., and Soifer, B.T., 1984. Astrophys. J. (Letters) **278**, L11.

Wang, R.T., 1980. In *Proceedings of the 1984 CSL Conference on Obscuration and Aerosol Research*, R.E Kohl, ed., p. 111.

Ward, L., 1988. *The Optical Constants of Bulk materials and Films*, Adam Hilger, Philedelphia.

Warren, S.G., 1984. Appl. Opt. **23**, 1206.

Warren, S.G., 1986. Appl. Opt. **25**, 2650.

Waterman, P.C., 1965. Proc. IEEE, **53**, 805.

Weiss-Wrana, K., 1983. Astron. Astrophys. **126**, 240.

Werby, M.F. and Chin-Bing, S.A., 1985. Comp. Math. with Appl. **11**, 717.

Wright, E.L., 1989. Preprint.

Yeh, C., 1964. Phys. Rev. **135**, A1193.

Yeh, C. and Mei, K.K., 1980. In *Light Scattering by Irregularly Shaped Particles*, D. Schuerman, (Ed.), Plenum, New York, p. 201.

Zerull, R.H., 1976. Beit. Phys. Atmos. **49**, 168.

Table 1

References of tabulated optical constants

Material	Reference
Amorphous carbon	Edoh, 1983; Huffman, 1988
Graphite	Draine, 1985; Querry, 1985
Magnetite	Huffman and Stapp, 1973; Steyer, 1974 Querry, 1985
Silicate, amorphous	Draine, 1975; Huffman and Stapp, 1973 Querry, 1984,1985,1986; Egan and Hilgeman, 1979 Palik, 1985
Silicate, crystalline	Steyer, 1974; Palik, 1985; Mukai and Koike, 1989
Water ice	Warren, 1984
Carbon dioxide ice	Warren, 1986
Tholins	Khare et. al, 1984; Khare et. al, 1987

Figure Captions

Figure 1. The real and imaginary index of refraction of magnetite Querry, 1984).

Figure 2. Representative behavior of the complex dielectric constant (top) and the complex index of refraction (middle) in the region of a *reststrahlen* band centered at ω_0. Also included is the reflectance spectrum from a normally incident beam and Q_{abs} for a $0.01\mu m$ grain.

Figure 3. Spectrum of real and imaginary indices of refraction for laboratory measurements of a composite clay with equal parts illite, montmorillonite, and kaolinite (Querry, 1984, thin line) along with the optical constants predicted from the Bruggeman theory (heavy line) using the optical constants from laboratory measurments of the individual minerals.

Figure 4. Log of the assumed phase function of P/Halley (Devine, et. al 1986), sampled every 30°, plotted against the log of the momentum transfer, q (see text). The straight line is a least squares fit to the data for scattering angles greater than 30°, and has a slope of which corresponds to a fractal dimension of 2.04.

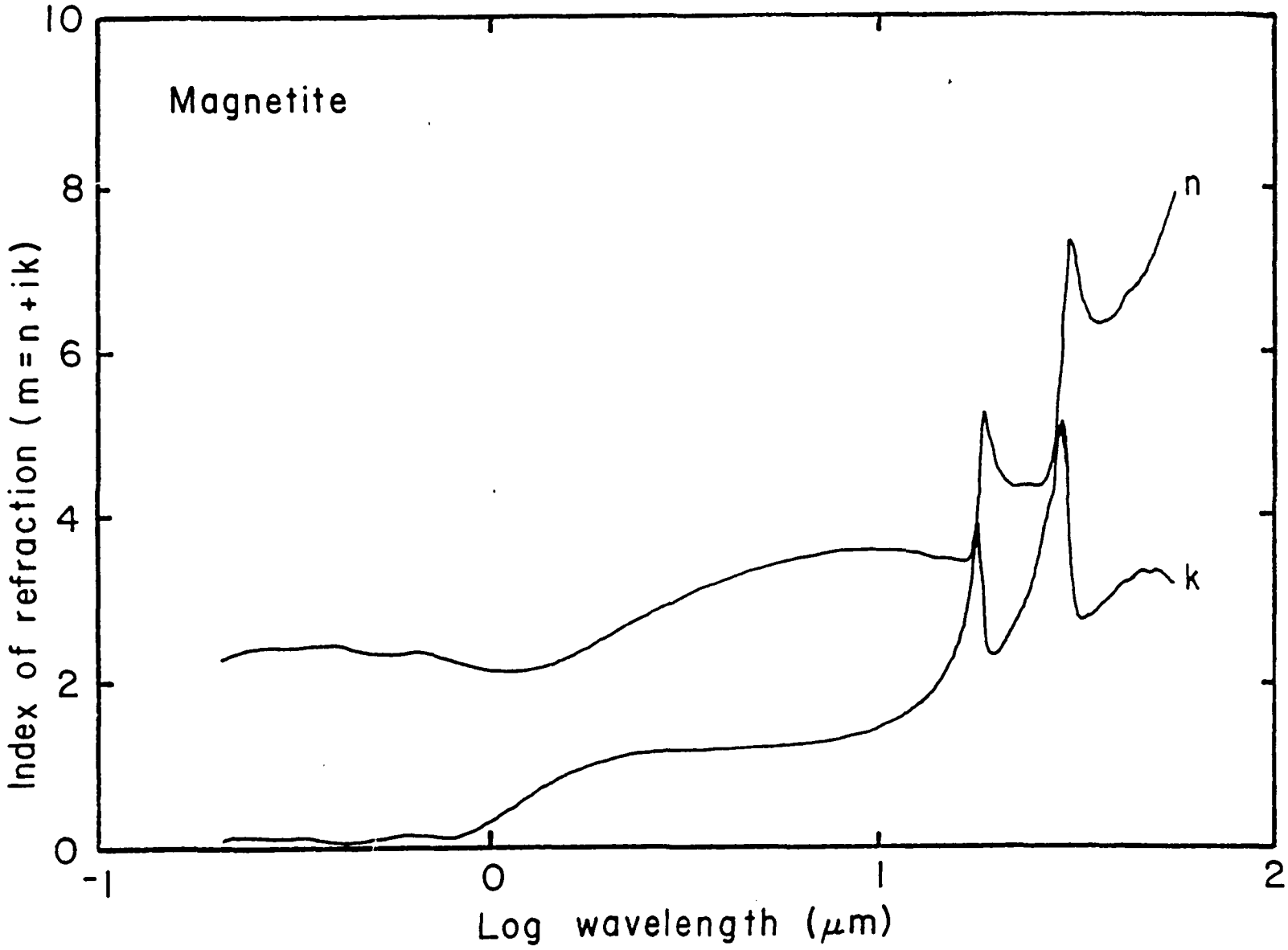
Magnetite
n
k
Index of refraction (m = n + ik)
Log wavelength (μm)
10
8
6
4
2
0
-1
0
1
2

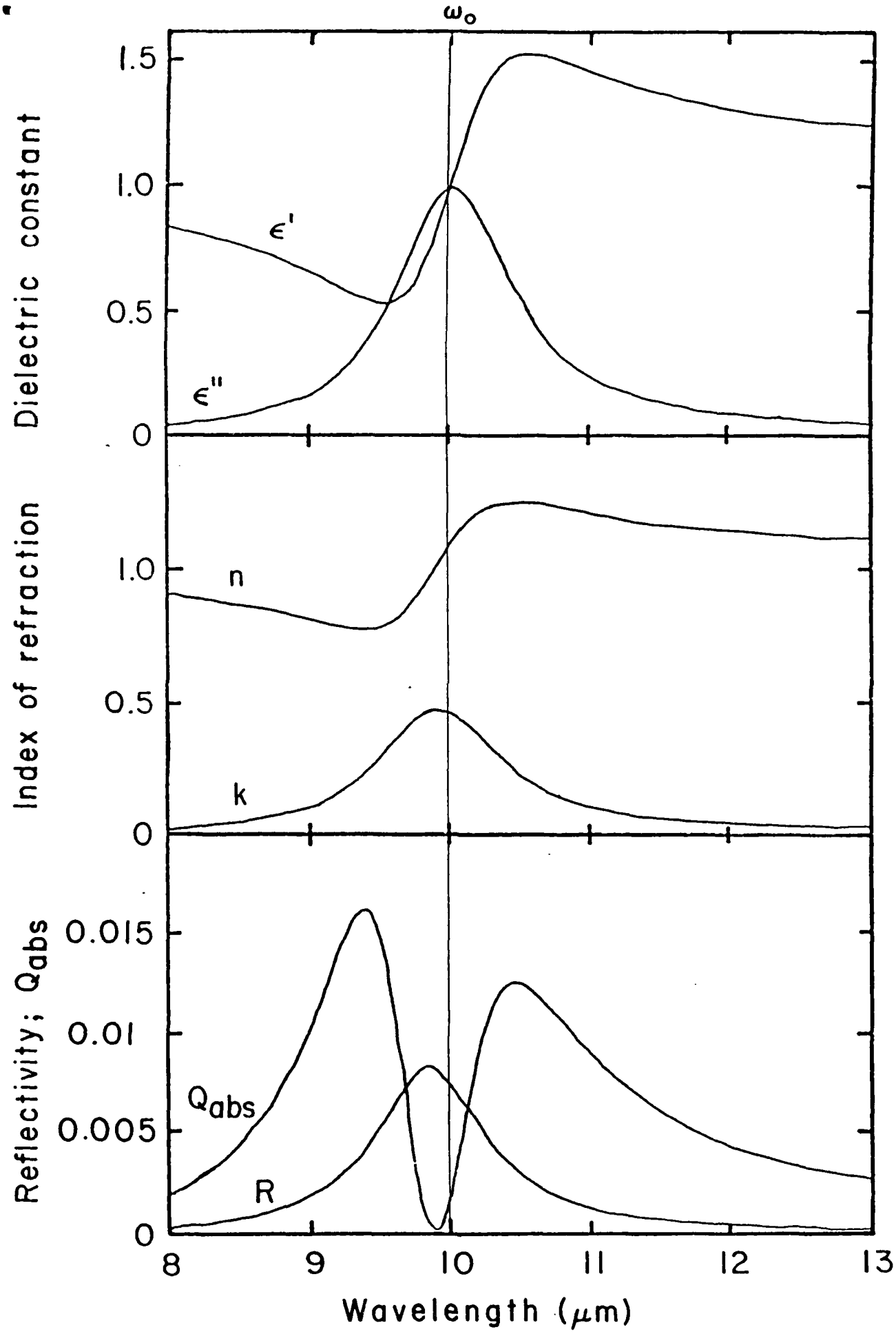
ω_o
1.5
1.0
0.5
0
Dielectric constant
ϵ'
ϵ''
1.0
0.5
0
Index of refraction
n
k
0.015
0.01
0.005
0
Reflectivity; Q_{abs}
Q_{abs}
R
8
9
10
11
12
13
Wavelength (μm)

Fig 2

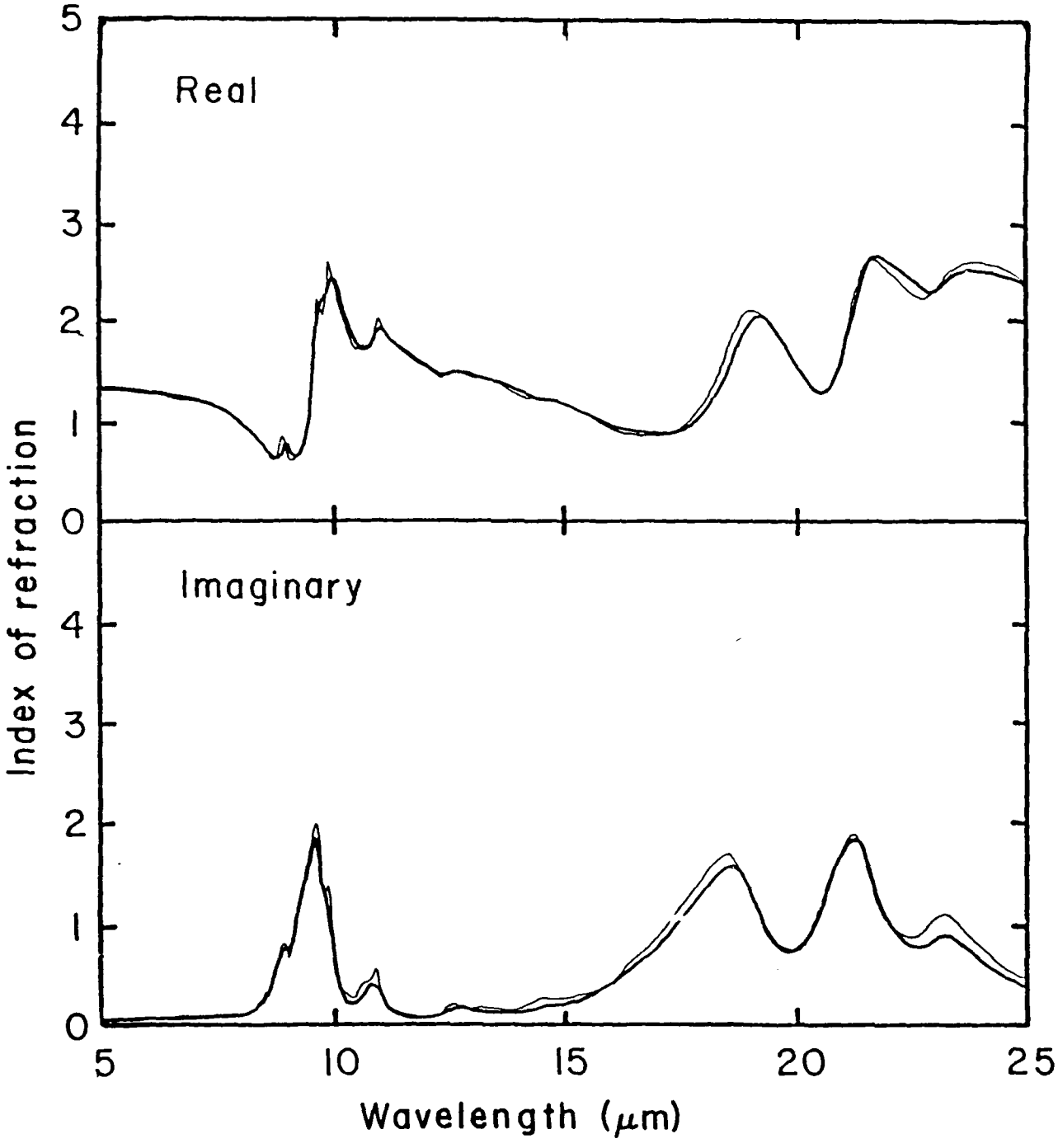
Real
Imaginary
Index of refraction
Wavelength (μm)
0
1
2
3
4
5
10
15
20
25

Fig 3

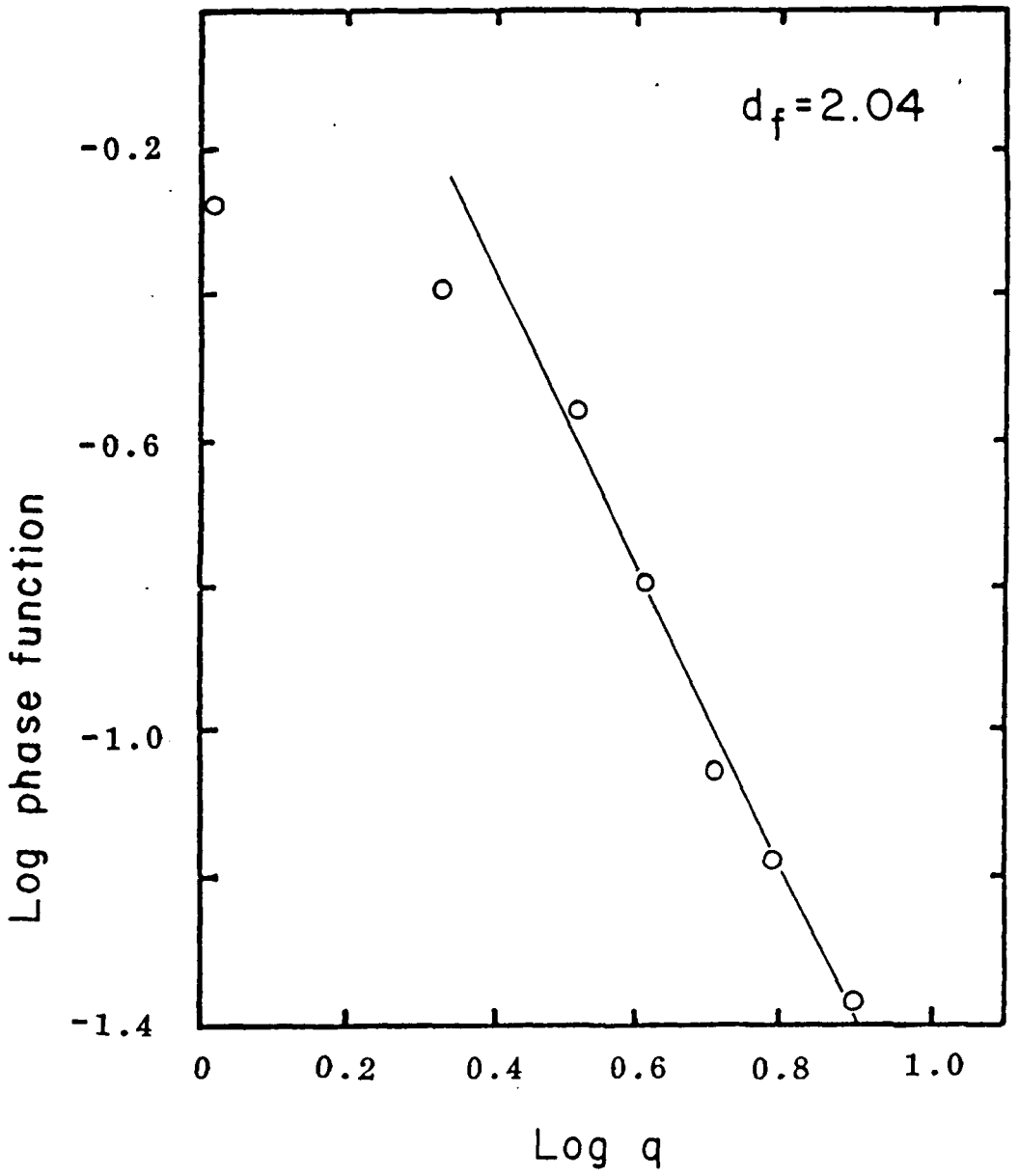
d_f=2.04
-0.2
-0.6
-1.0
-1.4
Log phase function
0
0.2
0.4
0.6
0.8
1.0
Log q